

Short Communication

## Pt Submonolayer Decorated PdAu/C Nanocatalyst for Oxygen Reduction Reaction

Weiping Li<sup>1,2,\*</sup>, Zhilu Le<sup>2</sup>, Tianxiang Zhou<sup>2</sup>, Mengyin Liao<sup>3,\*</sup>, Hesheng Liu<sup>1,2</sup>, Bing Na<sup>1</sup>, Yijun Yu<sup>2</sup>, Bin Wang<sup>1</sup>, Haiying Zhou<sup>1,2</sup>, Zhiliang Liao<sup>2</sup>, Keyi Zhang<sup>2</sup>

<sup>1</sup> Jiangxi Province Key Laboratory of Polymer Micro/Nano Manufacturing and Devices, East China University of Technology, Nanchang, 330013, China

<sup>2</sup> Jiangxi Engineering Research Center of Process and Equipment for New Energy, East China University of Technology, Nanchang 330013, China

<sup>3</sup> Institute of Energy Conversion, Jiangxi Academy of Sciences, Nanchang 330096, China

\*E-mail: [liweiping@ecit.cn](mailto:liweiping@ecit.cn) (Weiping Li); [lmy1324@126.com](mailto:lmy1324@126.com) (Mengyin Liao)

Received: 2 March 2018 / Accepted: 7 July 2018 / Published: 1 September 2018

---

We measured the activity of nanocatalyst, comprising Pt submonolayer decorated PdAu/C substrate (donoted as Pt-PdAu/C) with Pd/Au atomic ratio 4/1, in the oxygen reduction reaction in acidic media. The Pt-PdAu/C is synthesized via a spontaneous displacement reaction, which involves placing a small amount of Pt on carbon-supported PdAu nanoparticles. The decorated nanostructures are confirmed by an array of analytical techniques including transmission electron microscopy (TEM), X-ray diffraction (XRD) and X-ray photoelectron spectroscopy (XPS). Rotating disk electrode measurements show that the current density of Pt-PdAu/C nanocatalyst has 1.4 times higher than a commercial Pt/C for oxygen reduction reaction. The enhanced activity of the Pt-PdAu/C is derived from the combination of the synergistic effect of Pt submonolayer and of the PdAu alloy. Implications of these findings to the design of highly active low Pt loading nanocatalysts are discussed, along with their enhanced electrocatalytic performance in the fuel cell.

---

**Keywords:** Pt submonolayer, Oxygen reduction reaction, PdAu, Fuel Cells, Electrocatalyst.

### 1. INTRODUCTION

Proton exchange membrane fuel cells are drawing increasing attention due to high conversion efficiency, high power density, light weight, low pollution, and plenty of applications in automobiles, space shuttles, etc[1, 2]. However, the low catalytic activity of Pt towards the oxygen reduction reaction (ORR) and its high cost limit the wide application of this technology [3]. One common method to reduce the usage of Pt is to prepare a thin Pt layer on a less precious substrate metal. RR Adzic and co-workers deposited a Pt monolayer on the surface of substrate metal via copper underpotential deposition and galvanic replacement of Cu by Pt [4, 5] and it was found that the

utilization of Pt increases significantly because almost every Pt atom is on the surface of substrate metal and can take part in the electrocatalytic reactions. Moreover, the interactions between the Pt atomic monolayer and the substrate metal have been proved a synergistic effect upon improving ORR kinetics [6-8].

Inspired by the aboved results, many new approaches were developed to synthesize electrocatalysis for the ORR, which comprise Pt monolayer decorated precious metal alloys-, metal-, or core-shell-structures [9-11]. For example, RR Adzic and co-workers deposited a Pt monolayer via redox replacement of an underpotentially deposited Ru adlayer on the surface of the substrate metal [12]. The results show that almost every Pt atom takes part in the reaction, which results in greatly lowering Pt content. And higher Pt mass activity in ORR was found in all of the new electrocatalysts compared with those of commercial Pt/C electrocatalysts, which proved that this approach was successful. Lei and co-workers synthesized a Pd<sub>3</sub>Fe@Pt/C electrocatalyst with a novel core-shell structure for the oxygen reduction reaction, which deposited Pt onto the carbon enveloped Pd<sub>3</sub>Fe nanoparticles [13]. It was found that the Pd<sub>3</sub>Fe@Pt/C catalyst show a half-wave potential of 739 mV, which exhibits a shift of 21 mV more positive than that of Pt/C (718 mV) catalyst. In addition, in the oxygen reduction reaction, the Pd<sub>3</sub>Fe@Pt/C catalyst exhibited much better electrocatalytic performance than that of Pd<sub>3</sub>Fe/C and Pt/C catalyst. Yang and co-workers produced Pd@Pt nanoparticles on carbon with pseudo-core-shell structure and it was found that regardless of the total content of metal Pt or (Pd + Pt) is used as the basic normalization, the Pd<sub>70</sub>@Pt<sub>30</sub>/C catalyst always exhibits the highest activities, which are 1.22 and 2.8 times higher compared with Pt/C, respectively [14]. Therefore, the loading Pt in electrocatalysts can be reduced and deposited to one monolayer for the oxygen reduction reaction if with suitable substrate.

In this paper, new electrocatalyst synthesized via decorating a small quantity of Pt (monolayer-level) on carbon-supported PdAu alloy nanoparticles was prepared and investigated. The PdAu alloy particles were applied as substrate for the following surface displacement reaction of the Pt precursor in the solution and the metal constituents within the PdAu nanoparticles. The surface displacement reaction derives from the differences in equilibrium electrochemical potentials of the different redox couples, which include PtCl<sub>4</sub><sup>2-</sup>/Pt ( $E^0 = 0.775$  V vs. SHE), AuCl<sub>4</sub><sup>2-</sup>/Au ( $E^0 = 1.0$  V vs. a standard hydrogen electrode (SHE)), and PdCl<sub>4</sub><sup>2-</sup>/Pd ( $E^0 = 0.591$  V vs. SHE). Due to the differences described above, the outer layer Pd atoms within the PdAu alloy nanoparticles acted as sacrificing components for the reduction of Pt<sup>2+</sup> to Pt, resulting in the Pt deposition to the surface of PdAu nanoparticles at the expense of Pd. PdAu nanoparticles were selected as substrate due to their excellent chemical stability with acid resistance. This paper shows that the Pt-PdAu/C nanocatalyst possesses higher Pt activity than the commercial Pt/C electrocatalyst for the oxygen reduction reaction. The results provide a new method for further reducing the content of precious metal within electrocatalysts cathode for PEMFCs.

## 2. EXPERIMENTAL

### 2.1 Catalyst synthesis

Carbon supported PdAu alloy nanoparticles were obtained first by a modified two-phase method and the detailed preparation method has been described in our previous papers [15-18]. And

then a spontaneous displacement reaction between Pd atoms and  $\text{PtCl}_4^{2-}$  in the outer layer of the PdAu alloy nanoparticles was achieved to synthesize Pt decorated PdAu nanocatalyst. During the first step, an aqueous solution of  $\text{HAuCl}_4$  (0.066 g) and  $\text{PdCl}_2$  (0.114 g) was dissolved in a toluene solution of tetraoctylammonium bromide (1.1 g) to form a mixture with stirring. After 10 min stirring, the water phase was almost totally separated from the toluene phase. 2 mL oleylamine was then added to the toluene phase under stirring. In succession,  $\text{NaBH}_4$  (0.296 g, dissolved in 10 mL water) solution was rapidly added into the above suspension and the resulting suspension was further stirred for 4 h. Then ethanol (20 mL) was added to wash the PdAu nanoparticles and the mixture was precipitated out via centrifugation at 8000 rpm for 10 min. For the assembly of the PdAu nanoparticles on carbon support, 100 mg of carbon black (Vulcan® XC72R) were dispersed in 100 mL of hexane under sonication condition for 1 h and then followed by addition of the PdAu nanoparticles (20 mg of metals). The above mixture was stirred overnight at room temperature and the resulting product was obtained via centrifugation. The carbon-supported PdAu nanoparticles were collected and heated at 400°C under 10%  $\text{H}_2$  /90%  $\text{N}_2$  for 2h to remove the organic capping shell.

In the second step, 100 mg as-prepared carbon supported PdAu nanoparticles were submitted to another flask containing 20 mL deionized water and ultrasonicated for 30 min, 0.447mg of  $\text{K}_2\text{PtCl}_4$  aqueous solutions were added to the flask. After ultrasonically blending for 20 min, the mixture was conditioned at 80°C for 24 h with stirring. The obtaining powders were filtrated and then collected, after that, washed with deionized water until there is no chloride anion in the filtrate, and dried in the vacuum oven for 12 hours, by which the Pt-PdAu/C catalyst was obtained. The regulation of the Pt modification on the PdAu/C was realized by changing the ration of Pd/Pt mole.

## 2.2 Characterization

Transmission electron microscopy (TEM)(Technai F30 microscope) with an accelerating voltage of 300 kV was used to observe the nanostructure of the catalysts. The samples were prepared by ultrasonically dispersing the catalysts in ethanol and then putting the dispersed particles onto copper grids covered with a holey carbon film and then dried in air.

The X-ray diffraction (XRD) spectra of the catalysts' powder was obtained on a Panalytical X'Pert PRO X-ray diffractometer using  $\text{Cu K}\alpha$  radiation ( $k = 1.54056\text{\AA}$ ), operated at 40 kV and 30 mA. Diffraction patterns were collected from 30 to 90° at a scanning rate of 5° per minute, the step size is 0.02°.

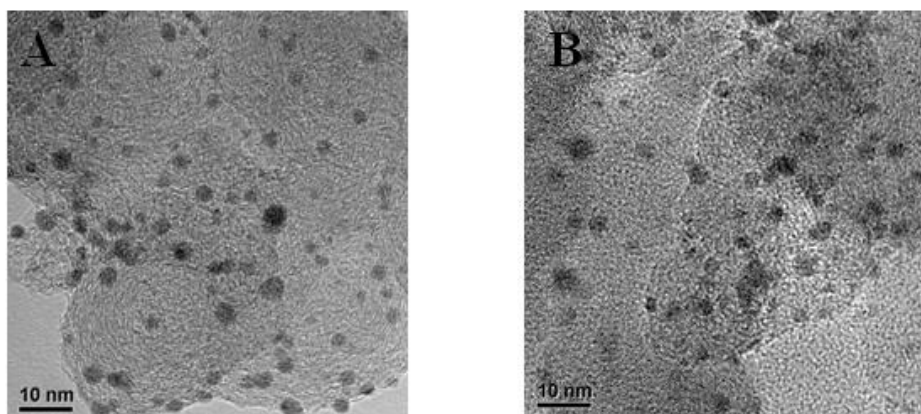
XPS characterization (PHI-Quantum 2000 spectrometer) was carried out to evaluate the surface composition and chemical conditions of the samples. Powder samples were pressed onto the wafer for subsequent test. Binding energies with referencing C1s at 284.6 eV were calibrated according to the previous reference [19].

An ordinary three-electrode experimental electrochemical cell was employed for tests [20]. The working three-electrode were prepared as follows: firstly, 10 mg of the as prepared catalyst powder was mixed with 20  $\mu\text{L}$  of a 0.25 wt % Nafion solution, which was diluted from a 5 wt % Nafion solution with ethanol (DuPont). Then, 5 mL of aqueous solution with 1 mL of isopropanol were added

in and mixed ultrasonically. Secondly, 10  $\mu\text{L}$  of the as prepared homogeneous catalyst solution was carefully transferred on a glassy carbon (GC) electrode and then dried at ambient temperature. Thirdly, negative-going linear sweep voltammograms were carried out with a Pt flag counter electrode, a freshly polished GC working electrode (4 mm, Pine Instruments), and a saturated calomel electrode reference electrode. All of the electrochemical tests were carried out at room temperature. The measurements of oxygen reduction reaction activities were conducted with 0.1 M  $\text{HClO}_4$  electrolyte. Negative-going linear sweep voltammograms were carried out from 0 V to 0.9 V at  $20 \text{ mV s}^{-1}$  in the presence of bubbling ultrapure oxygen to maintain a saturated oxygen atmosphere near the working electrode, more detailed information can be found in our previous work with reference [20].

### 3. RESULTS AND DISCUSSION

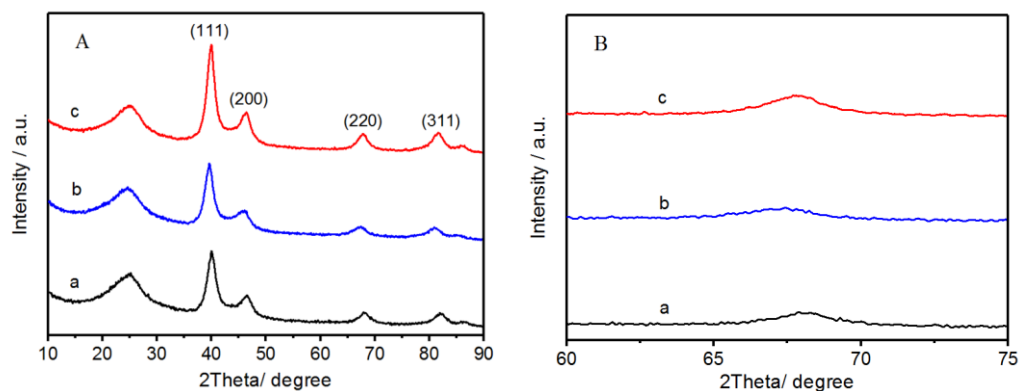
Figure 1 shows typical TEM images of the PdAu/C (A) and Pt-PdAu/C (B) nanocatalysts. It can be observed that the nanoparticles are fairly well dispersed on the carbon surface. The average particle size for PdAu/C and Pt-PdAu/C is  $5.5 \pm 0.7 \text{ nm}$  and  $5.6 \pm 0.6 \text{ nm}$ , respectively. Unfortunately, the decorated nanostructure is very difficult to be observed from the images of TEM. According to the principle of replacement reaction, the usage of  $\text{K}_2\text{PtCl}_4$  as the Pt precursor would not significantly alter the original structures, shapes, and sizes of the PdAu nanoparticles during our experiment. This result is differing from the case of using  $\text{Pt}^{4+}$  as precursor (such as  $\text{H}_2\text{PtCl}_6$  or  $\text{K}_2\text{PtCl}_6$ ), where one  $\text{Pt}^{4+}$  ion replace two Pd atoms and the larger Pt atoms displace the Pd atoms located in the core [15]. Hence, our experimental results agree well with other researcher's previous report.



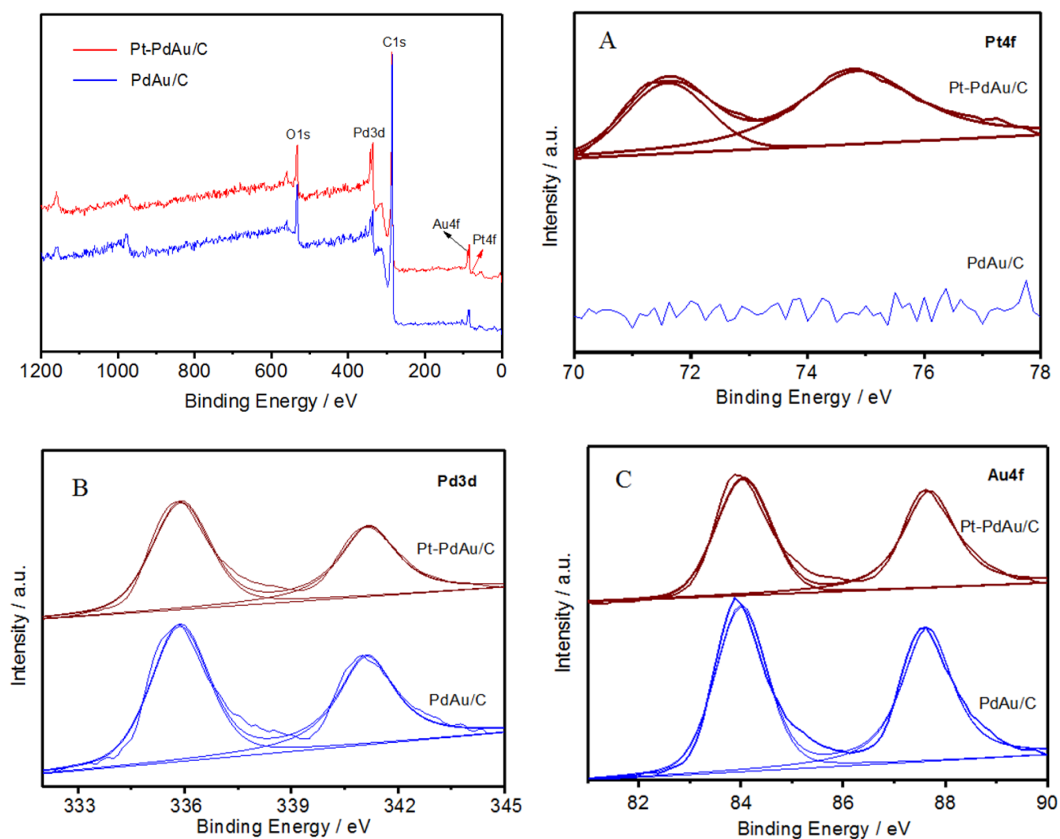
**Figure 1.** TEM images of (A) PdAu/C, and (B) Pt-PdAu/C(Pt:Pd=1:100) catalysts.

Figure 2A shows the XRD patterns of the Pd/C, PdAu/C and Pt-PdAu/C nanocatalysts. For all the catalysts samples, the peak at  $24.5^\circ$  is the characteristic of carbon support. The strong diffraction peaks at  $2\theta$  of  $39.7^\circ$ ,  $46.4^\circ$ ,  $67.7^\circ$ , and  $81.9^\circ$  are characteristic of face-centered cubic (fcc) Pd/C. It is interesting to found that the diffraction peak (220) for Pd/C, Pt-PdAu/C and PdAu/C catalysts (see Figure 2B), and that the peaks of Pt-PdAu/C and PdAu/C catalysts have a small negative shift in

comparison with that of Pd/C. Moreover, the lattice parameter of the Pd/C and PdAu/C is 0.3885 nm and 0.3930 nm, respectively, which were calculated according to Bragg's law [21] using (220) diffraction peak (at ca. 67.5°). These results agree well with the empirical values of the Pd/C (0.3880 nm) and the Pd<sub>80</sub>Au<sub>20</sub>/C (0.3921 nm) calculated by Vegard's law [22]. Hence, the XRD data prove that alloy structure is probably formed in the bimetallic PdAu nanoparticles.



**Figure 2.** XRD patterns. (A) XRD patterns for (a) Pd/C, (b) PdAu/C, (c) Pt-PdAu/C (Pt:Pd = 1:100) catalysts; (B) An enlarged image of the (220) diffraction peaks for different testing samples.



**Figure 3.** XPS survey scans of the Pt-Pd/C (Pt:Pd=1:100) catalyst; XPS spectra. (A) Pt 4f regions, (B) Pd 3d regions, (C) Au 4f regions for PdAu/C and Pt-PdAu/C (Pt:Pd=1:100) catalysts.

Figure 3 shows the XPS spectra of Pt-PdAu/C and PdAu/C nanocatalysts. The platinum peak in Pt-PdAu/C catalyst can be clearly observed whereas there is no platinum peak in PdAu/C catalyst (see Figure 3A), which indicates that the surface of the PdAu/C particles was covered by platinum. Moreover, the surface component calculated by the XPS analysis for the Pt-PdAu/C = 0.04:1:0.28 (atomic ratio), which clearly proves that much higher concentration of Pt was on the surface of Pt-PdAu/C alloy in comparison to that of atomic ratio of Pt to Pd being 1:100 in the precursor solution. Figure 3B and 3C shows the XPS spectra of Pd 3d and Au 4f in Pt-PdAu/C and PdAu/C, respectively. The binding energy of the Pd 3d and Au 4f peaks in Pt-PdAu/C is a little bit higher than those in PdAu/C. The binding energy shift may be attributed to the interaction between the Pt decorated atoms and PdAu alloy substrate.

Figure 4 displays the cyclic voltammograms of PdAu/C and Pt-PdAu/C nanocatalysts in 0.1 M HClO<sub>4</sub>. Typical hydrogen and oxygen adsorption/desorption behavior can be clearly observed on both PdAu/C and Pt-PdAu/C. Although the Pt-PdAu/C catalyst contained only a small amount of Pt, the hydrogen adsorption/desorption peak shape is similar to that of Pt/C [23]. It implies that most of PdAu surfaces had already been covered partly by Pt atoms, and that an interaction occurred between the PdAu substrate and the Pt in the surface. The peak at 0.5 V related to the reduction of Pt oxide, appear in Pt-PdAu/C sample, which affirms the presence of Pt in the Pt-PdAu/C nanocatalyst, and indicates that decoration with Pt could give rise to more hydroxyl species (OH<sub>ad</sub>) be absorbed by the catalyst.

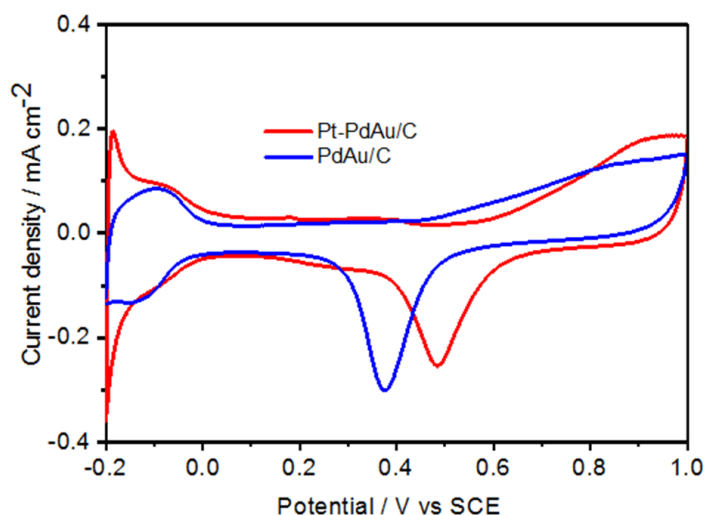


**Figure 4.** Cyclic voltammograms for PdAu/C and Pt-PdAu/C (Pt:Pd =1:100) catalysts in N<sub>2</sub>-saturated 0.1 M HClO<sub>4</sub> solution with a scan rate of 20 mV s<sup>-1</sup>.

The ORR on the precious metal surface has attracted much attention and is one of the most widely researched reactions in electrochemistry [24]. In this paper, main attention is focused on the performance in ORR in regard to their potential application as cathode catalysts used in PEMFCs. Figure 5A shows the ORR polarization curves for commercial Pt/C, PdAu/C and Pt-PdAu/C nanocatalysts in oxygen-saturated 0.1 M HClO<sub>4</sub> at ambient temperature with the potential range of 0-0.9 V. The activity of the Pt-PdAu/C catalyst is higher than that of the commercial Pt/C and PdAu/C

catalysts. And it is indicated that the curve produced in the case of the Pt-PdAu/C catalyst changes to a more positive value in comparison to that of the others on onset potential. Interestingly, the half-wave potentials of the Pt-PdAu/C catalyst is 0.618 V, which is a change of 23 mV more positive than that of the Pt/C (0.595 V) catalyst.

**Table 1.** the comparison of the prepared catalyst to those in the literature

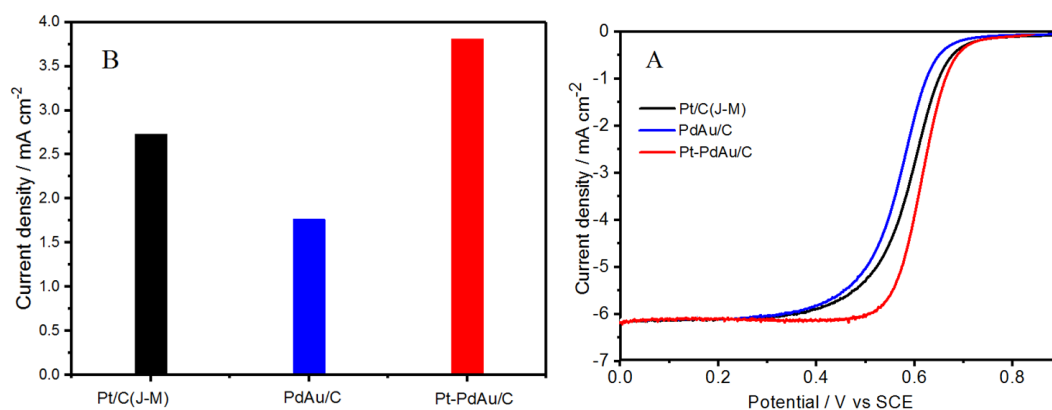
Authors	Catalyst types	Specific activity based on Pt/C	Ref.
RR Adzic	Re-Pt	4 and 4.5 times	12
RR Adzic	Pt/Pd <sub>3</sub> Fe/C	5 times	12
RR Adzic	Pt/Pd/C	3 times	12
ZQ Lei	Pd <sub>3</sub> Fe@Pt/C	1.06 times	13
JH Yang	Pd <sub>70</sub> @Pt <sub>30</sub> /C	1.22 and 2.8 times	14
Our work	Pt-PdAu/C	1.4 times	

Figure 5B shows the comparison of specific activities at 0.6 V with the Pt-PdAu/C, Pt/C and PdAu/C catalysts from RDE measurements at room temperature in this work. The plot shows that the specific activity of the Pt-PdAu/C (3.81 mA cm<sup>-2</sup>) catalyst is 1.4 times higher than that of the commercial Pt/C catalyst (2.72 mA cm<sup>-2</sup>).

In table 1 we make comparison the materials with similar electrocatalysts for ORR that were described in the reference literature. It can be seen from the table that compared with the catalysts listed in the literature, our catalysts prepared in this paper possesses several advantages as follows. Firstly, our catalysts were prepared with ultra-low content of precious metal Pt, which greatly lower the preparation cost. Secondly, the high acid resistant Au was added in our catalysts, which significantly increase the stability of the catalysts. Thirdly, our experimental results show that the catalysts exhibit appreciable catalytic activity compared with those in the literature.

The fact is that only surface atoms can take part in the catalyzing of the reaction, the experimental results can be explained by the fact that atoms of Pt on the surface of the PdAu substrate and the synergetic effect between the PdAu substrate and the Pt atoms. When Pt atoms are deposited on the other metal, then lattice expansion or compression might occur around the Pt layer because of the lattice mismatch. For instance, when Pt atoms are deposited on a Ru substrate, a compressive strain would occur, however, they a tensile strain would occur when deposited on Au substrate [25]. The metal substrate induced structural change could directly influence their electronic structure, which was indicated in their shifts of the d band [26-29]. As a result, binding of adsorbates onto Pt particles can be either weakened or reinforced, providing novel methods to tune the electrocatalytic activity for the Pt catalysts. Since Pt replaces Pd from the top layer, as a result the produced structure is overexpanded in the Pt-PdAu alloy surface leading to a little bit of compression is the most appropriate support substrate [30]. From Figure 3, the XPS data showed obvious evidence that the electronic effects come

out of Pt atoms with drawing electrons in the adjacent Pd atoms in the Pt-PdAu/C alloy, which indicates that the interaction between PdAu and Pt resulted from the favorable electronic effect could weaken the  $\text{OH}_{\text{ads}}$  binding. What's more, the strain in the Pt monolayer on another support substrate is considered to alter the monolayer's electronic properties, which leads to dramatic changes in the surface reactivity [31]. As a result, the nanocatalysts prepared in the paper may probably have something to do with the strain-induced electronic effect. Given the above, the Pt-PdAu/C alloy has shown their unprecedented high reactive activity for the oxygen reduction reaction.



**Figure 5.** (A) Linear voltammograms of commercial Pt/C, PdAu/C and Pt-PdAu/C (Pt:Pd =1:100) catalysts in  $\text{O}_2$ -saturated 0.1 M  $\text{HClO}_4$  showing the negative-going scans. Sweep rate:  $20 \text{ mV s}^{-1}$ , room temperature, and 1600 rpm. (C) Specific current density at 0.6 V for commercial Pt/C, PdAu/C and Pt-PdAu/C (Pt:Pd =1:100) catalysts.

#### 4. CONCLUSIONS

New nanocatalyst was synthesized via decorating a very little quantity of Pt on the carbon-supported PdAu nanoparticles. PdAu nanoparticles were precisely prepared by applying a modified double-phase protocol. Rotating disk electrode measurements revealed that the Pt-PdAu/C alloy nanocatalyst exhibited about 1.4 times higher in comparison to those of commercial Pt/C nanocatalyst. The observed high activity for Pt decorated was due to a decrease in the PtOH adsorption capacity because of the electronic interactions within the Pt atoms and PdAu substrate. Our experimental results indicate that it can be possible to construct the ORR nanocatalysts including only a very little bit of Pt atoms and a very little quantity of Pd atoms on the support substrate, the activity of which is much higher in comparison to that of the up to now carbon-supported Pt electrocatalysts. The significant improvement is ascribed to the surface decoration of the support substrate precious metal, as a consequent promoting their greatly increasing utilization. As a result, we can significantly lower the costs for the oxygen cathodes of the electrocatalysts.

#### ACKNOWLEDGEMENTS

The authors would like to thank the Natural Science Foundation of China (Grant NSFC 21663013), the Jiangxi Provincial Key Technology R&D Program (20161BBE50096), and the Jiangxi Provincial

Department of Education Technology R&D Program (GJJ150565) for financial supports. Part of work was supported by the Open Project Program of Jiangxi Engineering Research Center of Process and Equipment for New Energy, East China University of Technology

## References

1. C. J. Zhong, J. Luo, P. N. Njoki, D. Mott, B. Wanjala, R. Loukrakpam, S. Lim, L. Wang, B. Fang and Z. Xu, *Energy & Environmental Science*, 1 (2008) 454.
2. Y. J. Wang, N. Zhao, B. Fang, H. Li, X. T. Bi and H. Wang, *Chemical reviews*, 115 (2015) 3433.
3. K. Yasuda, A. Taniguchi, T. Akita, T. Ioroi and Z. Siroma, *Physical Chemistry Chemical Physics Pccp*, 8 (2006) 746.
4. J. Zhang, M. B. Vukmirovic, R. Klie, K. Sasaki, R. R. Adzic, *J. Phys. Chem. B*, 108 (2004) 10955–10964.
5. M. H. Shao, K. Sasaki, N. S. Marinkovic, L. Zhang, R. R. Adzic, *Electrochem. Commun.*, 9 (2007) 2848–2853.
6. J. Greeley, J. K. Norskov, M. Mavrikakis, *Annu. Rev. Phys. Chem.*, 53 (2002) 319–348.
7. Y. Xu, A. V. Ruban, M. Mavrikakis, *J. Am. Chem. Soc.*, 126 (2004) 4717–4725.
8. A. U. Nilekar, Y. Xu, J. Zhang, M. B. Vukmirovic, K. Sasaki, R. R. Adzic, M. Mavrikakis, *Top. Catal.*, 46 (2007) 276–284.
9. J. Zhang, M. B. Vukmirovic, K. Sasaki, F. Uribe and R. R. Adzic, *Journal of the Serbian Chemical Society*, 70 (2005).
10. J. Zhang, M. B. Vukmirovic, K. Sasaki, A. U. Nilekar, M. Mavrikakis and R. R. Adzic, *Journal of the American Chemical Society*, 127 (2005) 12480.
11. S. R. Brankovic, J. Mcbreen and R. R. Adžić, *Journal of Electroanalytical Chemistry*, 503 (2001) 99.
12. R. R. Adzic, J. Zhang, K. Sasaki, M. B. Vukmirovic, M. Shao, J. X. Wang, A. U. Nilekar, M. Mavrikakis, J. A. Valerio and F. Uribe, *Topics in Catalysis*, 46 (2007) 249.
13. W. Wang, R. Wang, S. Ji, H. Feng, H. Wang and Z. Lei, *Journal of Power Sources*, 195 (2010) 3498.
14. J. Yang, J. Lee, Q. Zhang, W. Zhou and Z. Liu, *Journal of the Electrochemical Society*, 155 (2008) B776–B781.
15. G. Chen, M. Liao, B. Yu, Y. Li, D. Wang, G. You, C. J. Zhong and B. H. Chen, *International Journal of Hydrogen Energy*, 37 (2012) 9959.
16. B. N. Wanjala, J. Luo, R. Loukrakpam, B. Fang, D. Mott, P. N. Njoki, M. Engelhard, H. R. Naslund, J. K. Wu and L. Wang, *Chemistry of Materials*, 22 (2010) 4282.
17. D. Mott, J. Luo, P. N. Njoki, Y. Lin, L. Wang and C. J. Zhong, *Catalysis Today*, 122 (2007) 378.
18. G. Chen, Y. Li, D. Wang, L. Zheng, G. You, C. J. Zhong, L. Yang, F. Cai, J. Cai and B. H. Chen, *Journal of Power Sources*, 196 (2011) 8323.
19. Q. Li, Y. Zhang, G. Chen, J. Fan, H. Lan and Y. Yang, *Journal of Catalysis*, 273 (2010) 167.
20. M. Liao, W. Li, X. Xi, C. Luo, Y. Fu, S. Gui, Z. Mai, H. Yan and C. Jiang, *International Journal of Hydrogen Energy*, 42 (2017) 24090.
21. V. J. L. Jenkins R., *John Wiley & Sons* (2012).
22. B. N. Wanjala, J. Luo, B. Fang, D. Mott and C. J. Zhong, *Journal of Materials Chemistry*, 21(2011) 4012.
23. Y. N. Wu, S. J. Liao, Z. X. Liang, L. J. Yang and R. F. Wang, *Journal of Power Sources*, 194 (2009) 805.
24. R. Srivastava, P. Mani, N. Hahn and P. Strasser, *Angewandte Chemie*, 46 (2007) 8988.
25. R. R. Adzic, J. Zhang, K. Sasaki, M. B. Vukmirovic, M. Shao, J. X. Wang, A. U. Nilekar, M. Mavrikakis, F. Uribe, *Top. Catal.*, 46 (2007) 249–262.

26. M. Mavrikakis, B. Hammer, J. K. Nørskov, *Phys. Rev. Lett.*, 81 (1998) 2819–2822.
27. L. Grabow, Y. Xu, M. Mavrikakis, *Phys. Chem. Chem. Phys.*, 8 (2006) 3369–3374.
28. T. Bligaard, J. K. Nørskov, *Electrochim. Acta*, 52 (2007) 5512–5516.
29. A. U. Nilekar, M. Mavrikakis, *Surf. Sci.*, 602 (2008) L89–L94.
30. J. R. Kitchin, J. K. Nørskov, M. A. Barteau, J. G. Chen, *J. Chem. Phys.*, 120 (2004) 10240–10246.
31. W. Yang, L. Zou, Q. Huang, Z. Zou, Y. Hu and H. Yang, *Journal of the Electrochemical Society*, 164 (2017) H331.

© 2018 The Authors. Published by ESG ([www.electrochemsci.org](http://www.electrochemsci.org)). This article is an open access article distributed under the terms and conditions of the Creative Commons Attribution license (<http://creativecommons.org/licenses/by/4.0/>).